Journal of Colloid and Interface Science 360 (2011) 132–138

Contents lists available at ScienceDirect

Journal of Colloid and Interface Science

www.elsevier.com/locate/jcis

Surface modification of alumina nanofibres for the selective adsorption of alachlor and imazaquin herbicides

Blain Paul, Wayde N. Martens, Ray L. Frost *

Discipline of Chemistry, Queensland University of Technology, Brisbane, Qld 4001, Australia

ARTICLE INFO

Article history:
Received 1 March 2011
Accepted 15 April 2011
Available online 27 April 2011

Keywords:
Grafted alumina fibres
Adsorption
Water purification
Herbicides
TEM

ABSTRACT

The effective removal of pollutants using a thermally and chemically stable substrate that has controllable absorption properties is a goal of water treatment. In this study, the surfaces of thin alumina (γ-Al_2O_3) nanofibres were modified by the grafting either of two organosilane agents, 3-chloro-propyl-triethoxysilane (CPTES) and octyl-triethoxysilane (OTES). These modified materials were then trialed as absorbents for the removal of two herbicides, alachlor and imazaquin from water. The formation of organic groups during the functionalisation process established super hydrophobic sites on the surfaces of the nanofibres. This super hydrophobic group is a kind of protruding adsorption site which facilitates the intimate contact with the pollutants. OTES grafted substrate were shown to be more selective for alachlor while imazaquin selectivity is shown by the CPTES grafted substrate. Kinetics studies revealed that imazaquin was rapidly adsorbed on CPTES-modified surfaces. However, the adsorption of alachlor by OTES grafted surface was achieved more slowly.

1. Introduction

There is concern about the existence of commercial herbicides in the environment due to the carcinogenic properties of these compounds. Herbicides are usually released into the environment through the industrial and agricultural operations resulting in them being detected in many surface and ground waters at extremely low concentrations. The removal of these compounds from water may be achieved with a variety of absorbents but the complete removal of these at low concentration is still somewhat difficult [1–9]. This study clearly illustrates that wide range of compounds with varied structures, sizes and functionality can be adsorbed effectively from aqueous systems only by the fine tuning of the adsorption sites [10–16]. It has also been seen that these pollutants exhibit different adsorption properties, with some being strongly adsorbed, whereas others are weakly adsorbed [1,3]. In general, the adsorption behaviour of adsorbents may be affected by many factors. Several investigators have evaluated the importance of the nature of the substrate and its functionalities during adsorption process [12,13,17]. Investigations have also been shown that the adsorption of certain solutes increases with an increase in the surface area of the substrate [18,19].

Porous solids such as activated carbon, natural clays and mesoporous silica possess very high surface area but are poor absorbents due to their the lack of favourable interaction with pollutants. In other words, when predicting the performance of absorbents, it is inadequate to explain the adsorption behaviour only by using the surface area of substrate. The presence of specific functional groups on the surface of the substrate imparts significant characteristics that enhance the adsorption of extremely low concentrations of pollutants. Many researchers have activated substrates by adding functional groups, extensive studies being reported for the adsorption of various pollutants using functionalised clays and mesoporous silica [20–27]. The dependence of the herbicide adsorption capacity of montmorillonite on the existence of pre-adsorbed micelles has been attributed to change in the characteristics of the adsorbents [28]. In some authors suggested the effect of coating on montmorillonite for the adsorption of simazine and its behaviour in solution in the process of adsorption [29]. Mesostructured silica has also been modified by the incorporation of cyclodextrin for use in the separation of aromatic molecules [30,31].

When an absorbent is chemically modified in such a way, it is difficult to maintain the stability of the internal pore structures or to get a steady flow rate through the internal channels of the material. The pores of many absorbents are in molecular dimensions so that pollutant molecules penetrating into the channels with bigger size are rejected from pores smaller than this size. When an absorbent is chemically modified, the modifying agent occupies the pore space thereby reducing the total pore volume and the pore diameter. This pore filling reduces the active area

* Corresponding author. Address: Queensland University of Technology, Faculty of Science and Technology, 2 George St., Brisbane, Qld 4001, Australia. Fax: +61 7 3138 1804.
E-mail address: r.frost@qut.edu.au (R.L. Frost).

0021-9797/$ - see front matter © 2011 Elsevier Inc. All rights reserved.
doi:10.1016/j.jcis.2011.04.055

for the absorption. On the other hand, the abundance of hydrophobic and protruding adsorption sites enhances the adsorption due to the favourable interaction between the modified sites and the sorbates [32]. In general, the formation of hydrophobic groups on the surface of the substrates during the functionalisation process increases the adsorptive capacity for many pollutants [4,5,8,33,34]. This increased hydrophobic nature can also reduce the preferential adsorption of water, and hence can prevent the blockage of the part of the surface and helps the surface directly interact with the pollutant molecules. It is therefore reasonable to expect that a stable substrate having certain critical structures and pore diameters can be functionalised with specific organic group leading to extremely high selective sorption capacity towards certain pollutants of low concentration while still maintaining an open porous network allowing high fluid flux.

Various types of oxide nanofibres have been extensively studied by researchers [35–39]. Thin nanofibres of γ-Al_2O_3 poses high surface area, high thermal and chemical stability and are easily modified on the surface with a large array of long chain organic functional moieties. In this study, the surface modification of γ-Al_2O_3 nanofibres by two different organosilane-grafting agents, 3-chloro-propyl-triethoxysilane (CPTES) and octyl-triethoxysilane (OTES), was undertaken and applied to the removal of alachlor and imazaquin from water.

2. Experimental section

2.1. Chemicals

The starting reagents for the preparation of γ-Al_2O_3 nanofibres were polyethylene oxide (PEO) surfactant (Tergitol 15S-7) and $NaAlO_2$ were purchased from Sigma–Aldrich which were both used as received. Acetic acid and hydrochloric acid were obtained from Merck. The organosilane-grafting agents 3-chloropropyltriethoxysilane (CPTES, 99%) and octyl-triethoxysilane (OTES, 99%) were purchased from Sigma–Aldrich and were used as served. All other reagents, unless otherwise stated, were used as received from Sigma–Aldrich except the toluene (99.8%), which was obtained from Merck and was used after drying (freshly distilled after keeping for 24 h in Na_2CO_3).

2.2. Preparation of γ-Al_2O_3 thin nanofibres and Grafting of functional groups

Thin γ-Al_2O_3 fibres were synthesized by a hydrothermal method and are denoted as AF. These fibres are 5–7 nm thick and 40–60 nm long with a specific surface area of 290 $m^2\,g^{-1}$. They were prepared by treating an aluminium hydroxide precipitate with a polyethylene oxide (PEO) surfactant (Tergitol 15S-7 from Aldrich) at 100 °C based on the reported work [37,38]. The reactions were performed in the following manner: 18.8 g of $NaAlO_2$ (0.2 mol of Al) was mixed with 50 mL of 5 M acetic acid solution with continual stirring. The obtained white precipitate was filtered and washed four times in order to remove residual Na ions (pH = 4–5). Aluminium hydrate cake obtained after washing was combined with 40 g PEO surfactant (chemical formula $C_{12-14}H_{25-29}O(CH_2CH_2O)_7H$ and an average molecular of weight 508) and stirred to homogenise thoroughly for 4 h. The sticky paste was transferred into a Teflon-lined stainless steel autoclave and heated in an oven at 100 °C. The molar ratio of $Al(OH)_3$/PEO/H_2O was 1:4:16. After 2 days, fresh aluminium hydrate cake was added to the heating mixture and was stirred for 30 min. The process of adding aluminium hydrate cake continued two more times during a period of 2 days. The final ratio of $Al(OH)_3$/PEO/H_2O was 5:1:8, 7.5:1:12 and 10:1:16, respectively, for each time. After 8 days of extensive heating in the oven, the reaction mixture led to the conversion of boehmite fibres. The phase transformation occurred during the calcination of boehmite fibres at 500 °C to γ-Al_2O_3 nanofibres.

Two different organosilane agents such as 3-chloropropyltriethoxysilane (CPTES) and octyl-triethoxysilane (OTES) were chosen to modify the surface after refluxing the γ-Al_2O_3 nanofibres in 0.2 M HCl for 6 h. The acid refluxed fibres are denoted as AF(A). The procedure used for the grafting of γ-Al_2O_3 fibres is described as follows: 1 g of acid treated fibres was placed in a 500 mL flask containing 60 mL dried toluene under stirring, 0.5 mL or 1 mL of CPTES (mass ratio, silane/alumina) was slowly added by means of a syringe. The mixture was refluxed at 120 °C for 48 h. After cooling, the product was filtered and washed several times with anhydrous enthanol to remove unreacted CPTES and then dried in a vacuum at 110 °C for 10 h. The resulting material was ground in a mortar and kept in a plastic tube for further characterization and utilization. The modified products were denoted as AFC1(50) (0.5 mL CPTES) and AFC1(100) (1 mL CPTES), respectively. Identical procedures were followed in the case of OTES except that the amount of OTES was 0.57 mL or 1.15 mL. The final materials were denoted as AFC8(50) (0.57 mL of OTES) and AFC8(100) (1.15 mL of OTES), respectively.

2.3. Adsorption test

The experiments were carried out using the batch equilibration method. For each determination, 20 mg of air-dried sample was mixed with 20 ml of alachlor with a concentration range of 2, 4, 6, 8 and 10 ppm, respectively, in different batches. Concentration ranges (1–5 ppm) were used for imazaquin. Due to the low rate of solubility of herbicides in water, the experiments were conducted in lower initial concentrations. The samples were equilibrated for 24 h at room temperature (23 °C) on a linear shaker in 50-ml polypropylene centrifuge tubes at neutral pH. Following equilibration, the samples were centrifuged and amounts of pollutants in the supernatant solutions were determined with Varian UV–Vis spectrophotometer Cary 100 with quartz 1-cm cuvettes. The absorbance of alachlor was monitored at 196 nm and imazaquin at 242 nm, respectively. Stock standard solution (2, 4, 6, 8, 10 ppm) of alachlor (1–5 ppm) was prepared and stored at room temperatures. The amount of herbicide adsorbed was determined by the difference in solution concentrations before and after equilibration. The entire tests performed were completely reproducible.

2.4. Characterization

XRD patterns were recorded using Cu Kα radiation (n = 1.5418 Å) on a Philips PANalytical X′ pert PRO diffractometer operation at 40 kV and 40 mA with 0.25° divergence slit, 0.5° antiscatter slit, between 5° and 90° (2θ). The FTIR spectra were acquired using Nicolet FTIR spectrometers Nicolet 380 equipped with Ge/KBr beamsplitter and dGTS/KBr detector. The collection time was about 1 min (64 scans) for background and sample. The spectrometer was purged with dry air. To prepare KBr pellets, about 2 mg of sample were taken, grinded 1–2 min together with about 200 mg of KBr (FT-IR grade, Fluka, dried). The pellets were pressed under vacuum for 4–6 min at 8t pressure to produce transparent discs about 1 mm thick and 13 mm in diameter. The samples were dried before preparation. An empty KBr pellet was used as reference and its spectrum was subtracted from the sample spectrum to suppress the spectral artefacts caused by KBr impurities and water. Thermal decomposition of the clay samples were carried out in an instrument incorporated with high-resolution thermo gravimetric analyser (series Q500) in a flowing nitrogen atmosphere (60 cm^3/min). Approximately 35 mg of each sample underwent thermal analysis, with a heating rate of 5 °C/min and

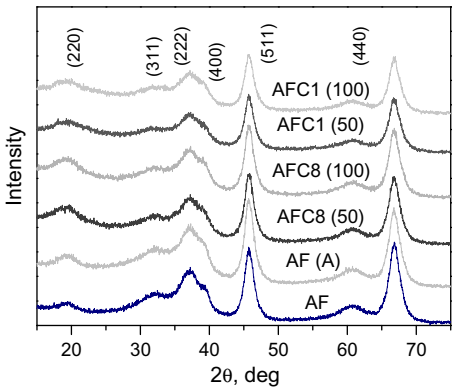

Fig. 1. XRD patterns of samples: AF – pure γ-Al_2O_3 fibres; AF(A) – acid washed fibres; AFC8(50) and AFC8(100) – OTES grafted samples; AFC1(50) and AFC1(100) CPTES grafted samples.

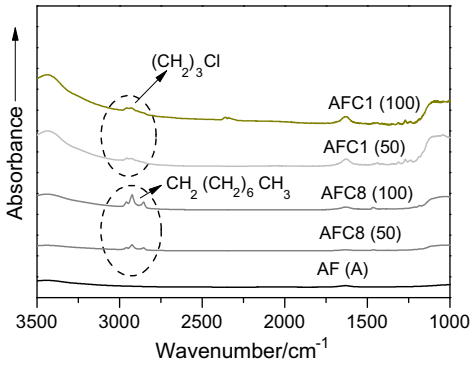

Fig. 2. FTIR spectra of samples: AF(A) – acid washed fibres; AFC8(50) and AFC8(100) – OTES grafted samples; AFC1(50) and AFC1(100) CPTES grafted samples.

with resolution of 6 from 35 °C to 1000 °C. Surface analysis based upon the N_2 adsorption/desorption technique was conducted on a micrometrics Tristar 3000 automated gas adsorption analyser after pre-treating the samples at 110 °C for 12 h under a flow of N_2. Contact Angle was analysed by Nanotech FTA200 Analyser. TEM images were taken using a Philips CM200 TEM with an accelerating voltage of 200 kV. The specimens were deposited onto a copper micro grid coated with a carbon film. Silica magic angle spinning (MAS) NMR spectra were acquired at a magnetic field of 9.4 T with a Varian 400 MHz spectrometer, operating at an excitation frequency of 79.4 MHz for ^{29}Si.

3. Results and discussion

3.1. X-ray diffraction and FTIR Spectra

Fig. 1 shows the XRD patterns before and after modification of γ-Al_2O_3 fibres. It can be seen from the XRD patterns that a slight decrease in peak sharpness was observed for the samples after grafting, indicating that there was slight changes in crystallinity after the grafting process. However, the overall crystal structure with and without grafting are similar. The standard XRD pattern of γ-Al_2O_3 from JCPDS cards (4-007-2479, 1-74-4629) were used in order to identify the diffraction lines. The calculation of unit cell dimensions indicated that unit cell parameters were not affected after grafting.

Fig. 2 displays the FTIR spectra of AF(A), AFC1 and AFC8. Samples AFC1 and AFC8 show bands in the 3000–2700 cm^{-1} region are found to be aliphatic C–H stretching vibrations [40]. Aliphatic CH_2 groups give rise to a doublet at 2938 and 2853 cm^{-1} in the AFC8 spectra, which is assigned to asymmetric and symmetric stretching, respectively.

3.2. TEM image

Fig. 3 shows the morphology of nanofibres before and after modification. As seen in the micrograph, functionalisation imparts the aggregation of fibres which can provide fibrillar interstices for the effectiveness of contact time and flow of contaminated water. Formations of these fibrillar interstices are important to improve the efficiency of the sorption.

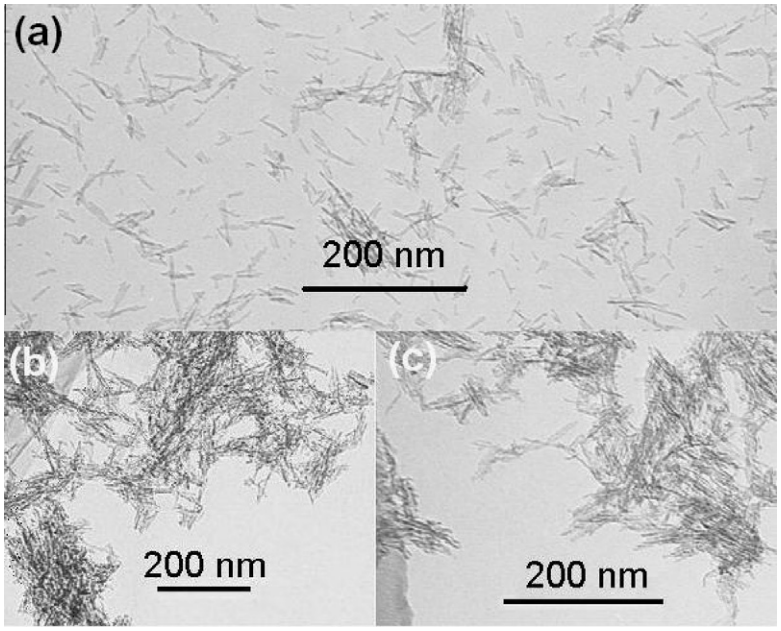

Fig. 3. (a) Transmission electron micrograph of AF(A); (b) and (c) micrographs of AFC8(100) and AFCI(100), respectively.

3.3. Thermogravimetric analysis

Fig. 4 shows the mass loss (TG) and the derivative mass loss (DTG) curves of γ-Al_2O_3 samples before and after modification. For the sample AF(A), the mass loss from 36–319 °C is assigned to chemically adsorbed water [38]. But in the case of the grafted samples, the stages of dehydration are partially overlapped with the decomposition of the organic species. The major mass loss is in the range of 211–704 °C for AFC8(100) corresponding to the DTG peak at 451 °C. This mass loss is assigned to the degradation of the organic groups. Sample AF(A) illustrated a slightly higher mass loss during the first stage due to the high amount of physically adsorbed water with less hydrophobic surfaces. For the OTES grafted sample AFC8(100), the first stage mass loss is 2% which corresponds to physically adsorbed water. The second stage of mass loss is associated with a very distinct peak and consists of the thermal decomposition of the organic species, which is about 14%. Almost similar mass loss was observed in the sample AFC1(100).

3.4. Nitrogen adsorption

The nitrogen adsorption isotherms of grafted samples are shown in Fig. 5. The isotherms of all the samples exhibit a type IV feature, corresponding to mesoporous materials with capillary condensation. The hysteresis of these samples exhibits the H3 hysteresis loop, which does not exhibit any limiting adsorption at high P/P_o, and is often observed with aggregates of plate-like particles giving rise to slit-shaped pores [41]. As seen in Fig. 5, the isotherm morphology of the grafted samples is similar to that of the non-grafted sample, suggesting the grafting process does not change the feature of the pore structure. However, with the increase in the ratio of organosilane to clay, the specific surface area and porous volume decrease, and the pore diameter slightly increases

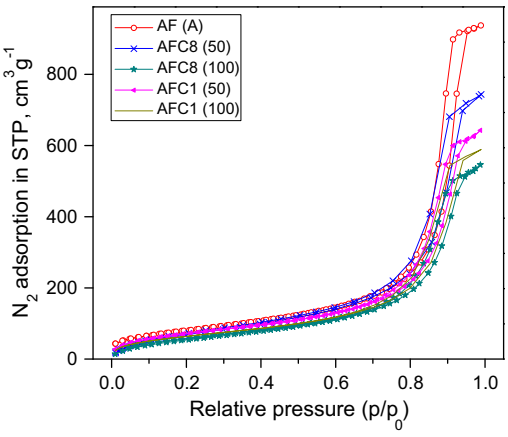

Fig. 5. N_2 adsorption/desorption isotherms for grafted and non-grafted γ-Al_2O_3 fibres: AF(A) – acid washed fibres; AFC8(50) and AFC8(100) – OTES grafted samples; AFC1(50) and AFC1(100) – CPTES grafted samples.

(Table 1). Apparently, the organic grafting reduces the surface area and the pore volume, which probably resulted from the grafting molecules occupying or blocking the interlayer spacing.

3.5. Contact angle

Fig. 6 shows the shape of a water droplet on the surface of the tablet form of γ-Al_2O_3 fibre samples. For the acid washed fibres, AF(A), water CA is as low as 18 ± 2° (Fig. 6a), displaying a hydrophilic surface. However, as shown in Fig. 6b and c, the water CA of the chloro-propyl group grafted fibres – AFC1(100) increased to 63 ± 2° and the value of octyl group grafted fibres – AFC8(100)

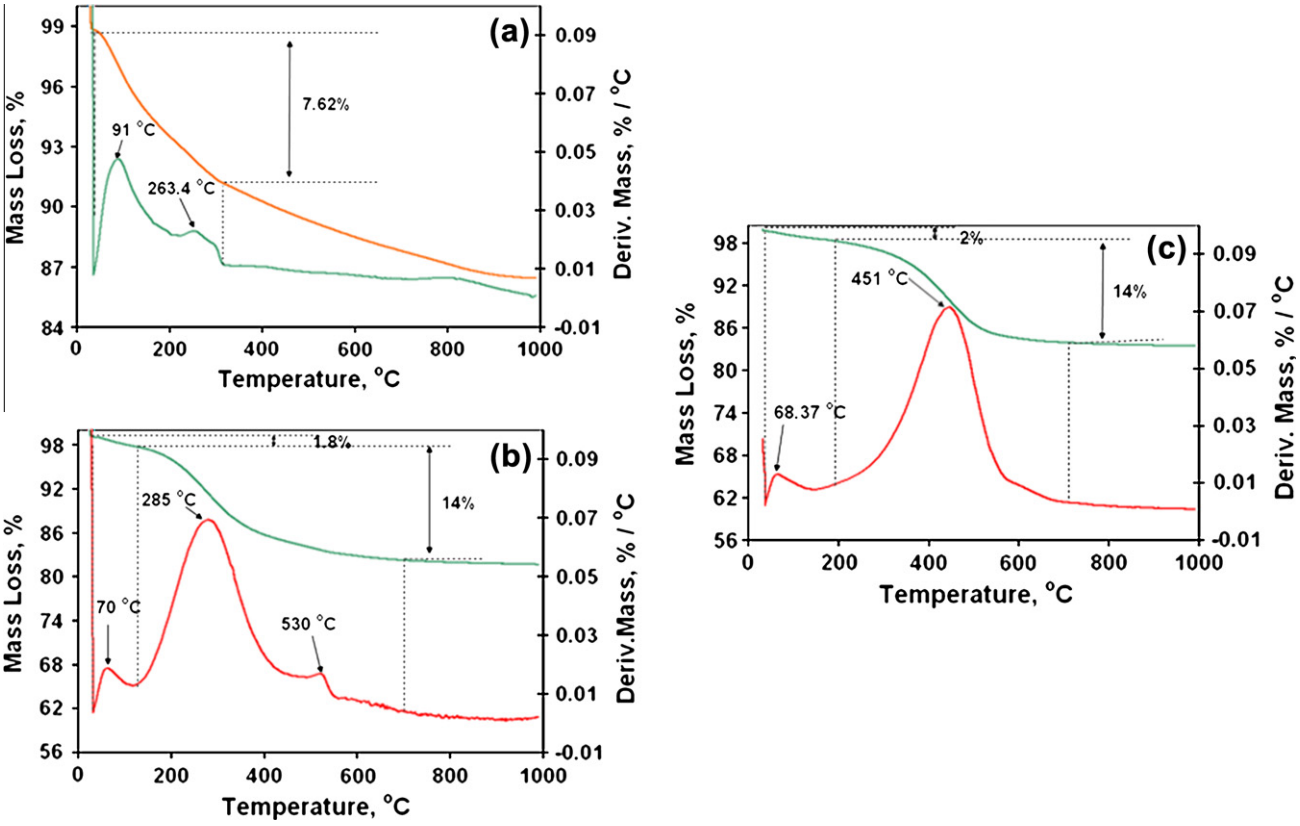

Fig. 4. Samples (a–c) are TGA and DTG curves of AF(A), AFC1(100) and AFC8(100) respectively.

Table 1
Specific surface area, pore volume and mean pore diameter of samples: AF and AF (A) as synthesized and acid washed γ-Al_2O_3, respectively; AFC8(50) and AFC8(100) – CPTES grafted samples; AFC1(50) and AFC1(100) – OTES grafted samples.

Samples	S_{BET} ($m^2\ g^{-1}$)	V_p[a] ($cm^3\ g^{-1}$)	Mean D [45]	
			BET[b]	BJH[c]
AF(F)	292	1.45	19.9	14.0
AFC1(50)	266	1	14.9	12.5
AFC1(100)	232	1	15.7	11
AFC8(50)	252	1	16.5	11.4
AFC8(100)	217	0.84	15.3	10.7

[a] Single-point adsorption total pore volume of pores at P/P_0 0.99.
[b] Adsorption average pore diameter (4 V/A by BET).
[c] Barrett–Joyner–Halenda (BJH) desorption average pore diameter (4 V/A).

is 146 ± 2°. Clearly, the surface modification of fibres leads to a significant change in the polar components therefore resulting in an increase in the contact angle.

3.6. Solid-state ^{29}Si MAS NMR spectra

The following discussion is based on the solid-state silicon-29 NMR spectra of modified γ-Al_2O_3 fibres. The formation of a different type of silica environment after grafting was confirmed by the solid-state ^{29}Si MAS NMR spectra (Fig. 7). The presence of T_1, T_2 and T_3 signals observed at −76, −67 and −58 corresponding to three different environments of silica atoms in all four samples [42]. T_1, T_2 and T_3 correspond to $[(CH_3CH_2O)_2[43]Si^*(CH_2)_3–Cl]$, $[CH_3CH_2O[43]_2Si^*(CH_2)_3–Cl]$ and $[AlO)_3Si^*(CH_2)_3–Cl]$, respectively, for the CPTES grafted γ-Al_2O_3 fibres. Furthermore, the OTES grafted γ-Al_2O_3 fibres, T_1, T_2 and T_3 are correspond to $[(CH_3CH_2O)_2[43]Si^*(CH_2)_7–CH_3]$, $[CH_3CH_2O[43]_2Si^*(CH_2)_7–CH_3]$ and $[AlO)_3Si^*(CH_2)_7–CH_3]$, respectively.

3.7. Adsorption of herbicides from water

Alachlor and imazaquin are two general use pesticides. The residual alachlor and imazaquin in water could cause environmental problems. The alumina nanofibres grafted with functional groups were used as sorbents to remove trace alachlor and imazaquin from water and is schematically represented in the Fig. 8.

The contact angle measurements show that the majority of the fibres surface was converted to a hydrophobic surface after the grafting process (Fig. 6). As a result, the hydrophobic region of the surface can make close proximity with the hydrophobic part of the adsorbed molecule. The main advantage of using fibre as absorbent was their easy separation from solutions after the adsorption process. Sorption isotherms of differently modified fibres were shown in Fig. 9. The grafted nanofibres exhibit a very high adsorption ability when compared with non-grafted γ-Al_2O_3

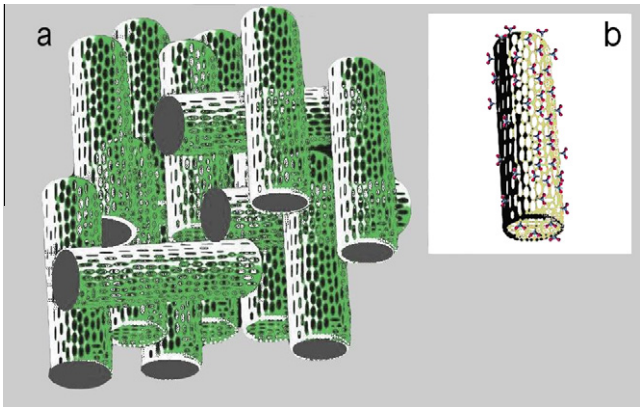

Fig. 8. The schematical diagrams of γ-Al_2O_3 fibres before (a) and after grafting (b).

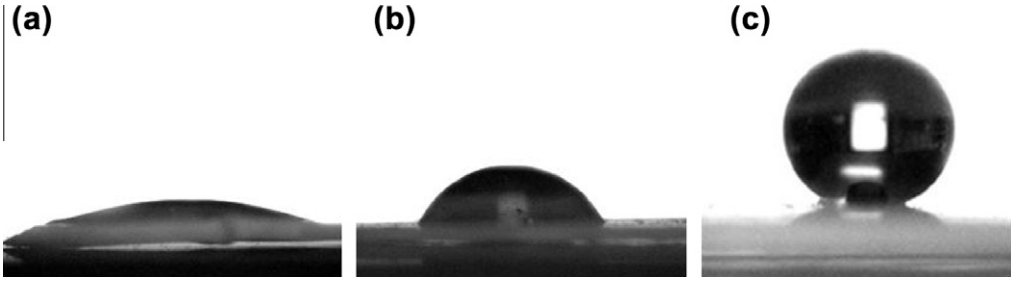

Fig. 6. The profile of water droplets on the surface of the pellets form of modified γ-Al_2O_3 fibres: (a) AF(A) – acid washed; (b) AFC1(100) – CPTES grafted samples; (c) AFC8(100) – OTES grafted samples, respectively.

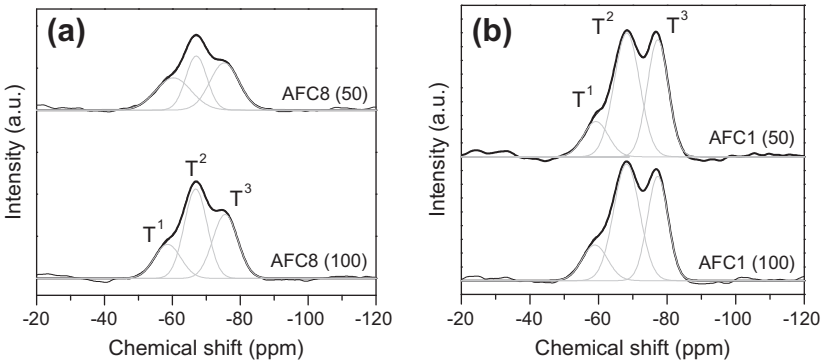

Fig. 7. Solid-state ^{29}Si MAS NMR spectra: (a) AFC8 – CPTES grafted samples; (b) AFC1 – OTES grafted samples.

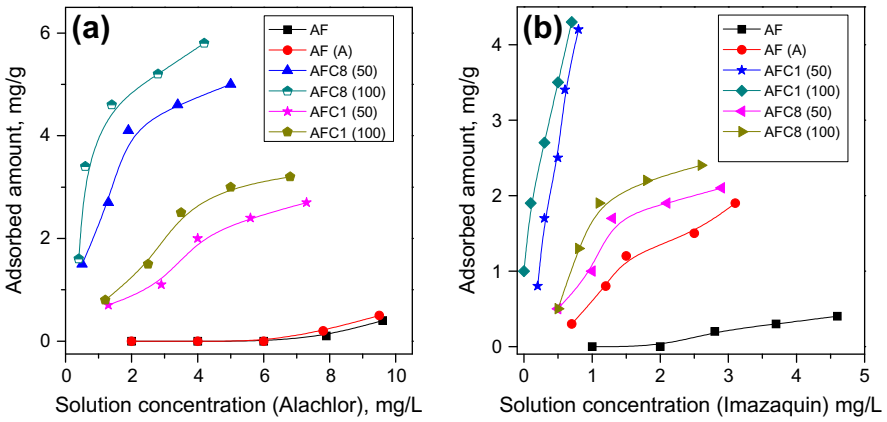

Fig. 9. Adsorption isotherms of alachlor (a) and imazaquin (b).

fibres. Sample AFC8(100) can absorb 1.6 mg/g alachlor at an initial lower amount of 2 mg/g and sample AFC1(100) can absorb imazaquin about 1 mg/g of adsorbent at an initial lower amount of 1 mg/g. It was also recognized that the rate of adsorption of imazaquin by CPTES was very high.

The linear part of the isotherms reflects the situation at low concentrations where the adsorption sites are far from being filled. The curves of the isotherms show that it becomes more difficult to adsorb additional molecules. As seen in Fig. 9, the adsorption isotherm of alachlor for AFC8(100) is also type H and the linearity of type C adsorption isotherm of imazaquin for AFC1(100) and AFC1(50) shows that the availability of more sites depend on how the adsorption proceeds [43]. The kinetics of uptake of the two pesticides was measured to evaluate the time needed to reach adsorption equilibrium. The rate of adsorption was measured by determining the change in concentration of the pollutants in contact with the adsorbent as a function of time. The sorbed amounts of pollutants were then plotted against the square root of time (Fig. 10).

Imazaquin was adsorbed readily by AFC1(100), reaching the adsorption equilibrium within 30 min whereas, a slow rate of adsorption was measured for alachlor by AFC8(100) with complete equilibrium being achieved only after 24 h. The adsorption mechanism is assumed to be proceeded in a multi-steps process. In the first step, the pollutant molecules transport from solution to the hydrophobic surfaces of alumina fibres. Secondly, the solute molecules diffuse into hydrophobic nanospaces; and finally, the adsorption process takes place. The small size of alachlor compared

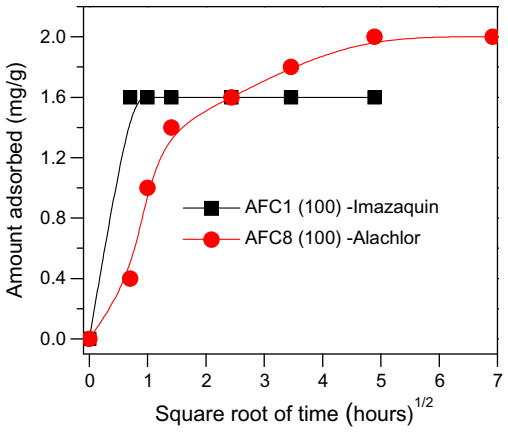

Fig. 10. The amount of uptake was plotted against the square root of time.

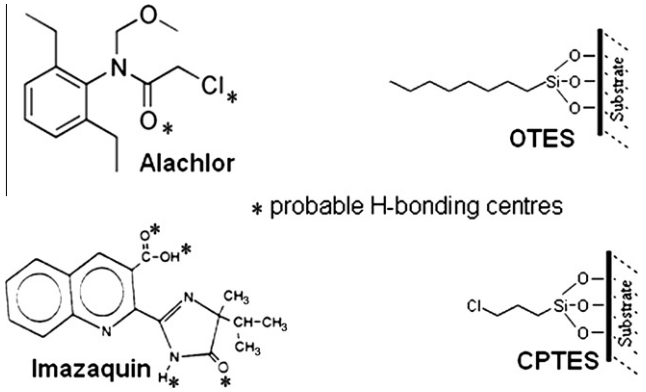

Fig. 11. A schematical view of grafted surface and possible interaction with pollutants.

with imazaquin, allows its easy adsorption onto the OTES grafted substrate which is mainly due to the hydrophobic interactions of the methyl groups present in the grafted species as well as in the alachlor molecules. Furthermore, molecules with larger number of hydrophobic alkyl groups are preferentially adsorbed. It is believed that the enhanced adsorption rate of imazaquin was determined by the hydrophobicity of alkyl groups as well as due to the large number of π bonding electrons in the imazaquin molecules. Hydrogen bonding plays a prominent role in the mechanism of the last step adsorption process (Fig. 11). It involves the interactions of aromatic π electron ring and the chlorine groups in a donor–acceptor mechanism take place through chlorine as an electron donor and an aromatic ring as the acceptor [44].

Intermolecular hydrogen bonds exist between the fibres providing cohesion of the fibrillar units. Indeed, these cohesive forces in the fibrillar interstices have a pronounced effect on the accessibility and the interactions of pollutants with the fibre. The aggregation of fibrils attributes the easy and high speed of the downstream separation.

4. Conclusions

Adsorption characteristics of functionalised thin γ-Al_2O_3 fibres were examined in batch processes. The efficiency of alachlor and imazaquin removal from water after grafting γ-Al_2O_3 fibres is significantly higher than that of non-grafted fibres. It was seen that these modified fibres exhibit different adsorption characteristics, i.e., some are strongly adsorbed whereas others are weakly

adsorbed depends on the functionalities. γ-Al_2O_3 fibres modified with OTES can absorb alachlor 1.6 mg/g of adsorbent at an initial lower concentration of 2 mg/g and CPTES grafted γ-Al_2O_3 fibres can absorb imazaquin about 1 mg/g of adsorbent at an initial concentration of 1 mg/g. A higher selectivity of imazaquin was observed for CPTES in comparison with OTES and an opposite effect was associated with alachlor uptake. After evaluating the kinetics of uptake, it was observed that CPTES grafted fibres could remove imazaquin much quicker than alachlor by OTES-modified substrate. The surface modification provided a relatively large number of highly hydrophobic sites and a super hydrophobicity was observed in the OTES system. Organically modified products were analysed by FTIR disclosed the existence of organic groups and also there is a significant decrease in the surface area after grafting by BET. XRD measurements indicated that grafting has no influence in the crystal structure of the substrate.

Acknowledgments

This work was supported by Australian Research Council (ARC). The author is grateful to Prof. H.Y. Zhu and Dr. Dongjiang Yang for their aid in the data analysis.

References

[1] S. Nir, T. Undabeytia, D. Yaron-Marcovich, Y. El-Nahhal, T. Polubesova, C. Serban, G. Rytwo, G. Lagaly, B. Rubin, Environ. Sci. Technol. 34 (2000) 1269–1274.
[2] T. Polubesova, Y. Chen, R. Navon, B. Chefetz, Environ. Sci. Technol. 42 (2008) 4797–4803.
[3] T. Polubesova, S. Nir, D. Zadaka, O. Rabinovitz, C. Serban, L. Groisman, B. Rubin, Environ. Sci. Technol. 39 (2005) 2343–2348.
[4] J.A. Smith, A. Galan, Environ. Sci. Technol. 29 (1995) 685–692.
[5] J.A. Smith, P.R. Jaffe, C.T. Chiou, Environ. Sci. Technol. 24 (1990) 1167–1172.
[6] J. Wei, G. Furrer, S. Kaufmann, R. Schulin, Environ. Sci. Technol. 35 (2001) 2226–2232.
[7] L. Zhu, B. Chen, X. Shen, Environ. Sci. Technol. 34 (2000) 468–475.
[8] J.A. Smith, P.R. Jaffe, J. Environ. Eng.-ASCE 120 (1994) 1559–1577.
[9] T. Polubesova, S. Nir, Z. Gerstl, M. Borisover, B. Rubin, J. Environ. Qual. 31 (2002) 1657–1664.
[10] F. De Juan, E. Ruiz-Hitzky, Adv. Mater. 12 (2000) 430–432.
[11] J.C. Dai, J.T. Huang, Appl. Clay Sci. 15 (1999) 51–65.
[12] L. Groisman, C. Rav-Acha, Z. Gerstl, U. Mingelgrin, Appl. Clay Sci. 24 (2004) 159–166.
[13] D. Zadaka, Y.G. Mishael, T. Polubesova, C. Serban, S. Nir, Appl. Clay Sci. 36 (2007) 174–181.
[14] K.A. Carrado, L.Q. Xu, R. Csencsits, J.V. Muntean, Chem. Mater. 13 (2001) 3766–3773.
[15] J.J. Tunney, C. Detellier, Chem. Mater. 5 (1993) 747–748.
[16] P.A. Wheeler, J.Z. Wang, J. Baker, L.J. Mathias, Chem. Mater. 17 (2005) 3012–3018.
[17] N. Masque, R.M. Marce, F. Borrull, J. Chromatogr. A 793 (1998) 257–263.
[18] D. Clifford, S. Subramonian, T.J. Sorg, Water treatment processes. III. Removing dissolved inorganic contaminants from water, Environ. Sci. Technol. 20 (2002) 1072–1080.
[19] S.B. Haderlein, K.W. Weissmahr, R.P. Schwarzenbach, Environ. Sci. Technol. 30 (1996) 612–622.
[20] R. Celis, M.C. Hermosin, J. Cornejo, Environ. Sci. Technol. 34 (2000) 4593–4599.
[21] L. Cox, R. Celis, M.C. Hermosin, J. Cornejo, A. Zsolnay, K. Zeller, Environ. Sci. Technol. 34 (2000) 4600–4605.
[22] X. Feng, G.E. Fryxell, L.Q. Wang, A.Y. Kim, J. Liu, K.M. Kemner, Science 276 (1997) 923–926.
[23] J. Liu, X.D. Feng, G.E. Fryxell, L.Q. Wang, A.Y. Kim, M.L. Gong, Adv. Mater. 10 (1998) 161–165.
[24] L. Mercier, T.J. Pinnavaia, Adv. Mater. 9 (1997) 500–503.
[25] H. Yoshitake, T. Yokoi, T. Tatsumi, Chem. Mater. 15 (2003) 1713–1721.
[26] J. Brown, L. Mercier, T.J. Pinnavaia, Chem. Commun. (1999) 69–70.
[27] A.M. Liu, K. Hidajat, S. Kawi, D.Y. Zhao, Chem. Commun. (2000) 1145–1146.
[28] T. Polubesova, S. Nir, D. Zadaka, O. Rabinovitz, C. Serban, L. Groisman, B. Rubin, Environ. Sci. Technol. 39 (2005) 2343–2348.
[29] F. Sannino, M.T. Filazzola, A. Violante, L. Gianfreda, Environ. Sci. Technol. 33 (1999) 4221–4225.
[30] R. Huq, L. Mercier, P.J. Kooyman, Chem. Mater. 13 (2001) 4512–4519.
[31] A. Bibby, L. Mercier, Green Chem. 5 (2003) 15–19.
[32] D.J. Yang, B. Paul, W.J. Xu, Y. Yuan, E.M. Liu, X.B. Ke, R.M. Wellard, C. Guo, Y. Xu, Y.H. Sun, H.Y. Zhu, Water Res. 44 (2010) 741–750.
[33] S.A. Boyd, M.M. Mortland, C.T. Chiou, Soil Sci. Soc. Am. J. 52 (1988) 652–657.
[34] J.A. Smith, P.R. Jaffe, Water Air Soil Pollut. 72 (1994) 205–211.
[35] H. Zhu, X. Gao, Y. Lan, D. Song, J. Am. Chem. Soc. 126 (2004) 8380–8381.
[36] S.C. Shen, Q. Chen, P.S. Chow, G.H. Tan, X.T. Zeng, Z. Wang, R.B.H. Tan, J. Phys. Chem. C 111 (2006) 700–707.
[37] H.Y. Zhu, X.P. Gao, D.Y. Song, Y.Q. Bai, S.P. Ringer, Z. Gao, Y.X. Xi, W. Martens, J.D. Riches, R.L. Frost, J. Phys. Chem. B 108 (2004) 4245–4247.
[38] H.Y. Zhu, J.D. Riches, J.C. Barry, Chem. Mater. 14 (2002) 2086–2093.
[39] Y. Xia, P. Yang, Adv. Mater. 15 (2003) 351–352.
[40] J.A. Gadsden, in: The Infrared Spectra of Minerals and Related Inorganic Compounds, Butterworth, London, 1975.
[41] S.J. Gregg, K.S.W. Sing, Adsorption, Surface Area and Porosity, second ed., Academic Press, New York, 1982.
[42] A. Shimojima, K. Kuroda, Angew. Chem. Int. Ed. 42 (2003) 4057–4060.
[43] C.H. Giles, T.H. MacEwan, S.N. Nakhwa, J. Chem. Soc. 5 (1960) 3973–3993.
[44] J.S. Mattson, H.B. Mark Jr., Activated Carbon-surface Chemistry and Adsorption from Solution, Marcel Dekker Inc., New York, 1971.
[45] R. Rajeswari, S. Kanmani, J. Sci. Ind. Res. 68 (2009) 1063–1067.